Chemical Science

Accepted Manuscript

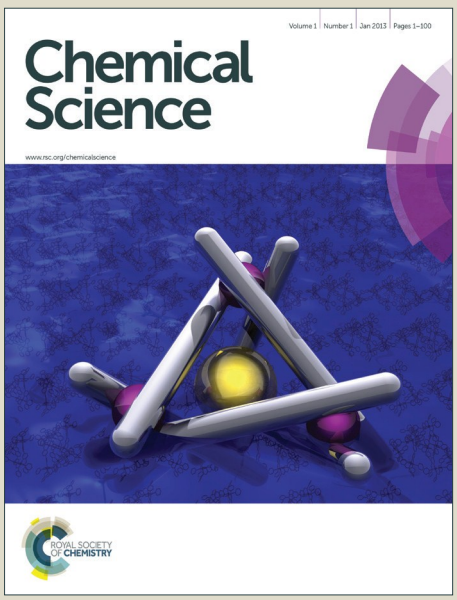

ROYAL SOCIETY OF CHEMISTRY

www.rsc.org/chemicalscience

Journal Name

ARTICLE

The impact of grafted surface defects and their controlled removal on supramolecular self-assembly

Received 00th January 20xx,
Accepted 00th January 20xx

DOI: 10.1039/x0xx00000x

www.rsc.org/

Ana M Bragança,[a] John Greenwood,[a]* Oleksandr Ivasenko,[a]* Thanh Hai Phan,[a,b] Klaus Müllen,[c] Steven De Feyter[a]*

We demonstrate the use of covalently modified graphite as a convenient and powerful test-bed for versatile investigation and control of 2-D crystallizations at liquid solid interface. Grafted aryls act as surface defects and create barriers to supramolecular self-assembly. Easily tunable grafting density allows varying the effect of such defects on supramolecular self-assembly. Finally, defects can be locally removed, triggering monolayer reconstructions and allowing *in-situ* investigations of thermodynamically unstable or metastable morphologies.

Introduction

Supramolecular self-assembly is an intensively studied topic and can be applied towards 2-D crystal engineering on atomically flat solid surfaces,[1-4] enabling the formation of multiple architectures with potential nanotechnology applications.[5-8] Control over the quality of molecular networks is a crucial necessity to tune surface or interfacial properties. This includes the formation of large defect-free crystals of organic semiconductors, which are important for high performance organic thin-film transistors.[9]

Common methods to control the quality of crystalline thin films on pristine and ideal surfaces include careful design of the building blocks[10] as well as finding optimal self-assembly conditions by varying the temperature,[11, 12] solute concentration,[13] type of solvent,[14, 15] solvent flow,[16] and substrate.[17] All of these parameters directly influence the nucleation, growth and/or ripening stages of 2-D crystallization. Surface defects might affect these processes though.

Surface defects are often inherent to surface systems. They can be the result of non-ideal production processes, including contamination, or are intrinsic to a material, and it may be impossible to avoid or remove them. These defects are often detrimental to the 2-D monolayer crystal quality and associated advantageous properties. They affect the quality of self-assembled monolayers by creating structural barriers to the formation of large domains. For example, the polycrystalline nature of a substrate is shown to induce grain boundaries and dislocations within a self-assembled monolayer.[18]

To gain insight into the role of defects and the way they affect 2-D crystallization, and to find ways to minimize their impact, it is important to come up with a test system that allows control of the surface defect density and to remove defects in a controlled fashion.

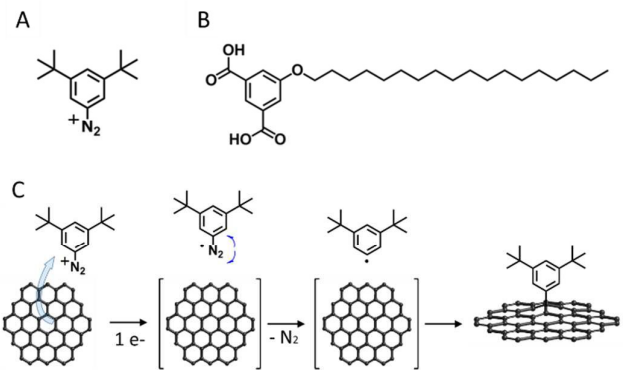

Figure 1. Molecular structure of: a) 3,5-bis-*tert*-butylbenzenediazonium (3,5-TBD), and b) 5-octadecyloxy-isophthalic acid (ISA-OC18). c) Reaction scheme for the generation and covalent attachment of 3,5-di-*tert*-butylphenyl radicals to the carbon surface.

In this study, by following a unique approach, we control the surface density of defects on graphite, and investigate the impact on monolayer nucleation and growth of a model molecular system. The defects are created by covalently grafting aryl radicals on the substrate, and their impact on 2-D crystal formation is probed using 5-octadecyloxy-isophthalic

[a] *Department of Chemistry, Division of Molecular Imaging and Photonics , KU Leuven-University of Leuven, Celestijnenlaan 200F, B-3001 Leuven, Belgium. E-mail: john.greenwood@kuleuven.be, oleksandr.ivasenko@kuleuven.be, steven.defeyter@kuleuven.be*
[b] *Department of Physics, Quynhon University, 170 An Duong Vuong, Quynhon, Vietnam*
[c] *Max Planck Institute for Polymer Research, 55128 Mainz, Germany*
Electronic Supplementary Information (ESI) available: description of data processing; assessment of the randomness of pin placement; influence of temperature; fractal analysis; STM nanolithography. See DOI: 10.1039/x0xx00000x

acid (ISA-OC18). The study reveals the importance of defect density and the various ways it impacts monolayer nucleation, growth, and ripening. We uncover the role of annealing in relation to defect densities. In addition, *in-situ* removal of individual grafted species enables control of 2-D crystallization processes with nanoscale precision. Our approach, using scanning tunneling microscopy (STM) as an imaging and nanolithography tool, provides novel opportunities to study and control self-assembly phenomena on surfaces.

Results and discussion

Recently, we have demonstrated that 3,5-di-*tert*-butylphenyl radicals (generated *via* electrochemical reduction of the corresponding aryldiazonium salt, 3,5-TBD, Fig. 1A,C) can covalently graft onto graphene and highly oriented pyrolytic graphite (HOPG).[19] Visualized with STM and atomic force microscopy (AFM), the grafted aryls appear as bright blobs (herein referred to as pins) 0.7 nm and 1-2 nm in height and width, respectively. The exact number of aryls within each pin is not known (most likely one or two).

Grafting appears to be random (see Section S2 in the supporting information), and the surface density of pins can be easily varied for a wide range of values. Grafted species have high stability and are not affected by the self-assembly of supramolecular building blocks at liquid-solid interface. Furthermore, we demonstrated that using very mild STM lithography pins can be locally removed with nanoscale resolution. These properties inspired us to test the applicability of such grafted surfaces in the investigation of 2-D crystallizations at liquid-solid interface.

As a model system for this study we chose 5-octadecyloxy-isophthalic acid (ISA-OC18, Fig. 1B). Its self-assembly on HOPG has been thoroughly investigated before,[20-23] allowing convenient selection of optimal conditions for self-assembly. The concentration of ISA-OC18 in octanoic acid solution was set to 0.2 mM. At room temperature (20°C) on bare HOPG, self-assembly yields ~1500-4000 nm^2 sized domains, easily distinguishable on large scale STM images (200 nm x 200 nm), shown in Fig. 2A. All domains belong to the same polymorph, consisting of H-bonded double-rows of isophthalic acid moieties and lamellar interdigitation of the alkoxy chains (Fig. 2B). Based on the surface density (ρ_N) of pins, all grafted samples were arbitrarily split into two groups: 1) samples with low surface density of pins (ρ_N =1500-6000 pins/μm^2, Fig. 2C), and 2) samples with high surface density of pins (ρ_N =13000-22000 pins/μm^2, Fig. 2D).

Upon adsorption, ISA-OC18 molecules assemble on grafted surfaces covering areas between pins. Since grafting is random, different combinations of pin/ISA-OC18 orientations are observed. In some cases pins are located inside of domains displacing few (2 to 6) ISA-OC18 molecules and disrupting normal H-bonding (Fig. 3A) and/or alkyl chain interdigitation (Fig. 3B) of the related lamellae. Occasionally, pins promote the formation of stacking faults (Fig. 3C) that propagate over several lamellae within the domain. Grouped together, several pins can create large holes in 2-D crystals (Fig. 3D). Finally, many pins are localized at the inter-domain borders (Fig. 3E).

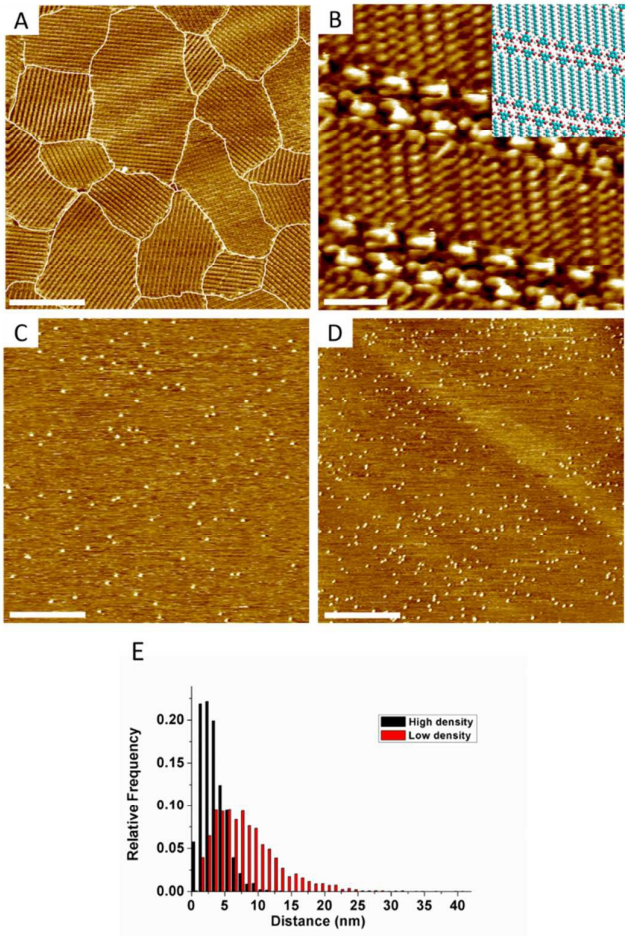

Figure 2. STM images of: a) ISA-OC18 (0.2 mM) self-assembly, at 20 °C, on bare HOPG (V_s = -0.700V, I_t = 80 pA, scale bar = 50 nm), b) close up view together with molecular model (inset) of ISA-OC18 self-assembly (V_s = -0.675 V, I_t = 100 pA, scale bar = 1.5 nm). HOPG samples with c) low-density (V_s = -0.700 V, I_t = 80 pA, scale bar = 50 nm), and d) high-density grafting (V_s = -0.700 V, I_t = 70 pA, scale bar = 50 nm). e) Histogram revealing the distributions of the nearest-neighbour distances of pins on HOPG with low- and high-density grafting.

The ability of a 2-D crystal to grow around defect sites decreases when the number of randomly distributed defects increases. To demonstrate this, we compared ISA-OC18 assemblies on the samples with low (ρ_N =1500-6000 pins/μm^2, Fig. 4A) and high (ρ_N =13000-22000 pins/μm^2, Fig. 4B) surface density of defects. The histogram in Fig. 4C shows the difference is quite dramatic: while low grafting does not markedly affect the size distribution of ISA-OC18 domains compared to ISA-OC18 self-assembly at 20°C on bare HOPG (occasionally reaching 10000 nm^2), highly grafted samples contain much smaller domains (<3000 nm^2, with majority ≤1000 nm^2).

The contrasting results obtained using the pristine and grafted samples need to be considered in the context of the different stages involved in 2-D crystal growth. Similar to bulk

crystallization of materials, self-assembly of molecules at the solution-solid interface also proceeds in three distinct stages; namely, nucleation, free growth, and ripening.[24] Nucleation involves adsorption of molecules from the solution onto the surface followed by their 2-D diffusion to form small islands.

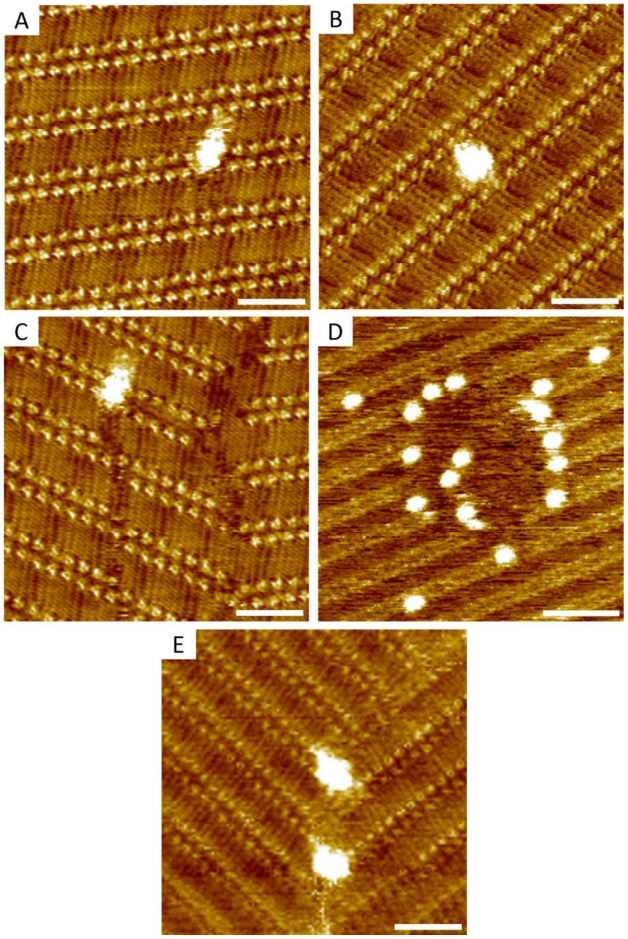

Figure 3. STM images of different combinations of pins/ISA-OC18 interactions: pins inside the domains disrupting a) H-bonding (V_s = -0.700 V, I_t = 80 pA, scale bar = 4 nm) or b) alkyl chain interdigitation (V_s = -0.700 V, I_t = 79 pA, scale bar = 4 nm); pins causing c) stacking faults (V_s = -0.700 V, I_t = 80 pA, scale bar = 4 nm) or d) holes within the domain (V_s = -0.675 V, I_t = 80 pA, scale bar = 8 nm); pins located at e) the inter-domain borders (V_s = -0.710 V, I_t = 80 pA, scale bar = 4 nm).

This highly dynamic process involves constant formation and dissolution of molecular islands until they reach a certain critical size above which the rate of formation is larger than the rate of dissolution. Nucleation is followed by free growth of the domains, where molecules are added to growing crystallites.

When the whole surface is covered, free growth is not possible and domains can become larger only by consuming neighboring domains. At low temperatures, the ripening step is slow, and it is often sufficient to only consider the nucleation and free growth step to describe the outcome of self-assembly.[25] The increased number of pins, as well as the lowered distance between them (Fig. 2E) in the samples with high grafting density, makes arrays of pins to act as barriers slowing down the domain growth (see also Section S3 in the supporting information). Consequently, new crystals nucleate on yet uncovered substrate, eventually yielding a monolayer composed of many small domains. The results of a dedicated investigation of the nucleation of ISA-OC18 on grafted surfaces will be reported elsewhere.

Even though at low grafting density the grafted aryls do not induce any significant alteration to the number of domains, it would be a mistake to think that the pins are inactive. They also limit the maximum size of domains that can grow. The only reason why this was not apparent is that at 20°C domains do not grow larger even on defect-free HOPG. To support this statement, we performed experiments at 25°C. In this case, a temperature difference of only 5°C was enough to promote the formation of very large domains of ISA-OC18 assemblies on bare HOPG (Fig. 5A). This is understandable since increasing temperature simultaneously decreases the probability of nucleation and increases the rates of free growth. Yet when the same self-assembly occurred on the samples with low grafting density, 2-D growth was limited by the defects (Fig. 5B), showing very similar domain size distribution to the one observed on the low density grafted samples at 20°C (see the supporting information, Fig. S2).

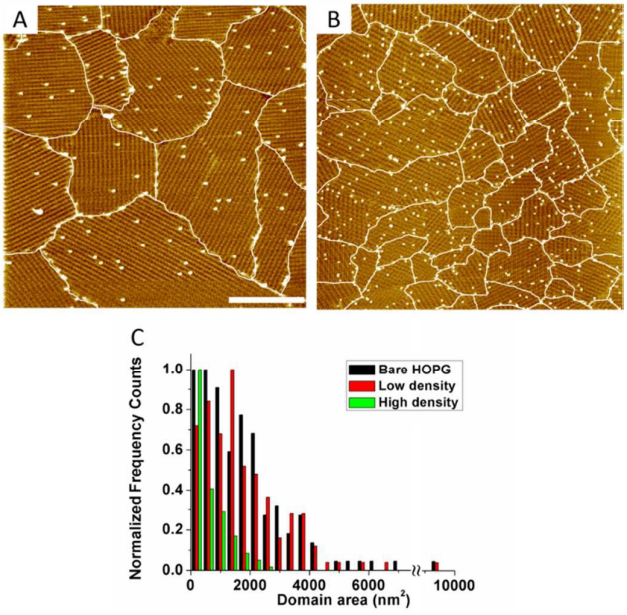

Figure 4. STM images of ISA-OC18 (0.2 mM) self-assembly, at 20 °C, on modified HOPG with a) low (V_s = -0.700 V, I_t = 80 pA, scale bar = 50 nm) and b) and high density of grafted species on the surface (V_s = -0.800 V, I_t = 80 pA, scale bar = 50 nm). c) Histogram revealing the domain size distribution of ISA-OC18 self-assembly on bare and modified (both grafting regimes) HOPG samples, at 20 °C.

So far, we have seen the influence of defects on the nucleation and growth of ISA-OC18 assemblies. To observe ripening of 2-D crystals we have to anneal the assembly at higher temperatures since at ambient temperatures ripening of these assemblies is too slow to follow with STM. For this, the assemblies formed at 20°C were annealed for 5 minutes at 60°C, cooled down to 20°C and imaged. Short annealing time prevented significant solvent evaporation. Grafted aryls remain unaltered, yet significant

reconstruction of ISA-OC18 self-assembly occurred. On the samples with low surface density of pins the domains grow very large (≥40000 nm^2), with the majority of pins being inside domains (Fig. 5C), causing only minor disruption of intermolecular interactions within isolated lamellae; as also observed in Figs. 3A and B. Annealing ISA-OC18 self-assembly on the samples with high surface density of pins also resulted in the ripening of domains (Fig. 5D). Here, however, very large domains (>40000nm^2) are rare and, instead, the domains are significantly smaller and spread in size over a rather wide range (200 – 15000 nm^2, see supporting information Fig. S3). This is the direct consequence of very small nearest neighbor distances (2-15 nm, Fig. 2E) between pins in these samples and the randomness of grafting. Interestingly, pin defects do not seem to complicate the shape of domains- just make them smaller (see Section S6 in the supporting information). Thus, suitably grafted samples can be effectively used to slow down growth and ripening stages in 2-D crystallizations.

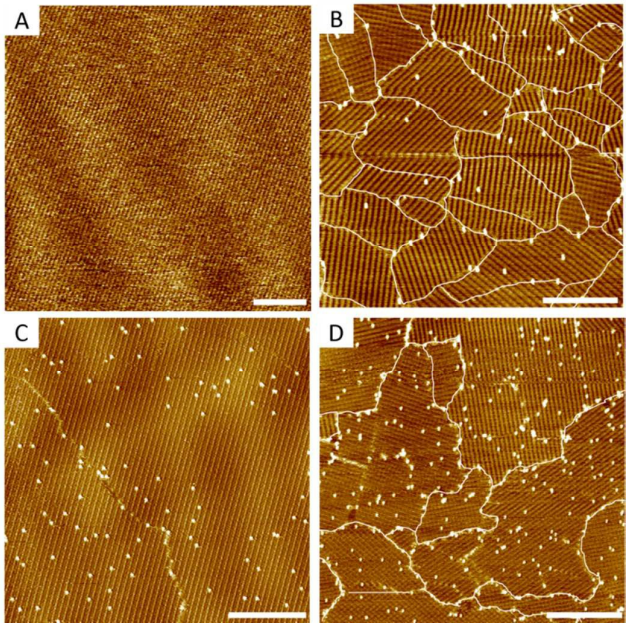

Figure 5. (a,b) STM images of ISA-OC18 (0.2 mM), self-assembly formed at 25ºC, on: a) bare HOPG (V_s = -0.775 V, I_t = 90 pA, scale bar = 50 nm), b) modified HOPG with a low density of grafted species (V_s = -0.700 V, I_t = 100 pA, scale bar = 50 nm). (c,d) STM images of ISA-OC18 (0.2 mM), with self-assembly formed at 20ºC, annealed at 60ºC for 5 min and imaged after cooling back to 20ºC: c) on modified HOPG with a low density of grafted species (V_s = -0.700 V, I_t = 80 pA, scale bar = 50 nm), d) on modified HOPG with a high density of grafted species (V_s = -0.700 V, I_t = 80 pA, scale bar = 50 nm).

In addition to the ease of introduction, the high control over the degree of surface modification and the robustness of the defect sites, grafted aryls can be removed selectively and with nanometer precision.[19] This makes arylated substrates very powerful test-beds for different experiments at the nanoscale. For example, the local removal of pins in selected areas (marked with white squares in Figs. 6A and 6C) results in room temperature ripening of the relevant domains and only within the degrafted region (Figs. 6B and 6D).

The reconstruction is fast and is driven by the minimization of the thermodynamically unstable inter-domain borders. The outcome: large domains grow at the expense of the smaller ones (Ostwald ripening). Interestingly, it appears that the sequence in which the pins are removed (for now this has only been done by controlling the scanning direction during degrafting) defines which domains will compete, and in what order. The STM precision is sufficient to remove a single pin without affecting its neighbors (see supplementary information, Fig. S4). Thus, using lithographic scripts, it should be possible to program any removal sequence of designated pins. The applicability and limitations of this idea are currently under investigation.

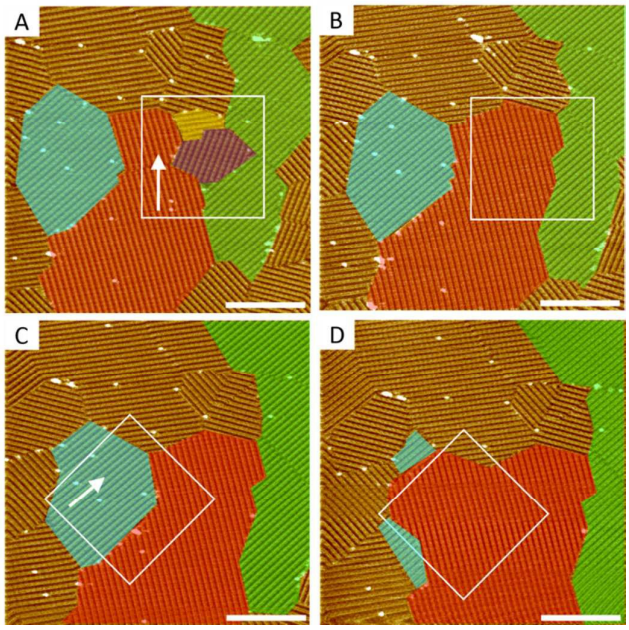

Figure 6. STM images of ISA-OC18 (0.2 mM) on modified HOPG with a low density of grafted species where pins enclosed within the marked areas (white squares) a) and c) were locally removed using mild STM lithography conditions (V_s = -0.001 V, I_t = 200 pA). Ostwald ripening followed in the degrafted zones b) and d) in the next scan (V_s = -0.720 V, I_t = 70 pA, scale bar = 40 nm).

Conclusions

We have investigated self-assembly of 5-octadecyloxy-isophthalic acid (ISA-OC18) on arylated graphite at the liquid-solid interface. Grafted aryls (pins) act as surface defects: They locally disrupt supramolecular networks, and can alter nucleation, growth, and ripening of 2-D crystals. The use of covalently grafted surfaces allows for tuning the morphology of self-assembled monolayers, creating polycrystalline surfaces with improved thermal stability. The ability to remove defects selectively with nanometer precision was used to follow localized Ostwald ripening, triggered by *in-situ* degrafting of selected pins. Ease of grafting, chemical robustness and selective degrafting makes covalently arylated HOPG a powerful test-bed for advanced characterization of 2-D crystallizations at the nanoscale.

Experimental section

Scanning tunneling microscopy

Small amounts (~12 µL) of ISA-OC18 solutions were drop-casted onto the basal (0001) plane of freshly cleaved highly oriented pyrolytic graphite (HOPG, grade ZYB, Advanced Ceramics Inc., Cleveland, OH, U.S.A.) and visualized with scanning tunneling microscopy (STM - PicoLE (Agilent) or a Molecular Imaging STM system) in constant current mode. The tips were mechanically cut from Pt/Ir (80/20, ⌀ 0.25 mm) wire. Several samples were investigated, and for each sample, several locations were probed. The bias voltage refers to the substrate. STM data analysis was performed using WSxM 5.0.40 and scanning probe image processor (SPIP) software (Image Metrology ApS). High-resolution images were corrected for drift using the recorded graphite images for calibration purposes allowing a more accurate unit cell determination.

Electrochemical measurements and grafting protocol

All electrochemical measurements were performed using an Autolab PGSTAT101 potentiostat (Metrohm_Autolab BV, The Netherlands). Prior to each experiment, the HOPG electrode was freshly cleaved using scotch tape. The electrochemical modification of the HOPG samples was carried out in a lab-built single-compartment three-electrode cell, with a working electrode area of 38.5 mm^2, Pt wire counter and Ag/AgCl/ 3 M NaCl reference electrodes. 3,5-Bis-*tert*-butylbenzenediazonium (3,5-TBD) is unstable, and decomposes rapidly; hence, it was synthesized from the aniline precursor immediately prior to electrochemical reduction. 3,5-Bis-tert-butylaniline (98%) was purchased from TCI-Tokyo Chemical Industry Co., Ltd. and used without further purification. 5 mL of 3,5-bis-tert-butylaniline (0.05-0.2 mM and 0.4 mM for low-density and high-density grafting, respectively) in 0.05 M HCl aq were mixed with aqueous $NaNO_2$ (0.1 mL, 0.1 M), and after approximately 3 min the mixture was injected into the electrochemical cell to run cyclic voltammetry (3 cycles, range: 0.5V to -0.6V, scanning rate: 100mV/s). After modification, the 3,5-TBD modified HOPG samples were rinsed with Milli-Q water to remove any physisorbed material from the surface, and dried in a stream of argon. The grafting density varied both within and between samples, hence we found it more reliable to split grafting into two categories (low (ρ_N =1500-6000 pins/μm^2 and high ρ_N =13000-22000 pins/μm^2) by directly analyzing the surface density of pins in the STM images.

Acknowledgements

This work is supported by the Fund of Scientific Research–Flanders (FWO), KU Leuven Internal Funds, and Belgian Federal Science Policy Office (IAP-7/05). The research leading to these results has also received funding from the European Research Council under the European Union's Seventh Framework Programme (FP7/2007-2013)/ERC Grant Agreement no. 340324.

Notes and references

1. J. A. Theobald, N. S. Oxtoby, M. A. Phillips, N. R. Champness and P. H. Beton, *Nature*, 2003, **424**, 1029-1031.
2. Y. Xue and M. B. Zimmt, *J. Am. Chem. Soc.*, 2012, **134**, 4513-4516.
3. M. O. Blunt, J. C. Russell, M. d. C. Giménez-López, J. P. Garrahan, X. Lin, M. Schröder, N. R. Champness and P. H. Beton, *Science*, 2008, **322**, 1077-1081.
4. J. A. A. W. Elemans, S. Lei and S. De Feyter, *Angew. Chem., Int. Ed.*, 2009, **48**, 7298-7332.
5. M. Blunt, X. Lin, M. d. C. Gimenez-Lopez, M. Schroder, N. R. Champness and P. H. Beton, *Chem. Commun.*, 2008, DOI: 10.1039/B801267A, 2304-2306.
6. S. J. H. Griessl, M. Lackinger, F. Jamitzky, T. Markert, M. Hietschold and W. M. Heckl, *Langmuir*, 2004, **20**, 9403-9407.
7. D. Wu, K. Deng, Q. Zeng and C. Wang, *J. Phys. Chem. B*, 2005, **109**, 22296-22300.
8. J. M. MacLeod, O. Ivasenko, C. Fu, T. Taerum, F. Rosei and D. F. Perepichka, *J. Am. Chem. Soc.*, 2009, **131**, 16844-16850.
9. D. Cahen, A. Kahn and E. Umbach, *Mater. Today*, 2005, **8**, 32-41.
10. M. Lackinger, S. Griessl, T. Markert, F. Jamitzky and W. M. Heckl, *J. Phys. Chem. B*, 2004, **108**, 13652-13655.
11. M. O. Blunt, J. Adisoejoso, K. Tahara, K. Katayama, M. Van der Auweraer, Y. Tobe and S. De Feyter, *J. Am. Chem. Soc.*, 2013, **135**, 12068-12075.
12. C. Marie, F. Silly, L. Tortech, K. Müllen and D. Fichou, *ACS Nano*, 2010, **4**, 1288-1292.
13. F. Silly, *J. Phys. Chem. C*, 2012, **116**, 10029-10032.
14. W. Mamdouh, H. Uji-i, J. S. Ladislaw, A. E. Dulcey, V. Percec, F. C. De Schryver and S. De Feyter, *J. Am. Chem. Soc.*, 2006, **128**, 317-325.
15. X. Zhang, T. Chen, Q. Chen, G.-J. Deng, Q.-H. Fan and L.-J. Wan, *Chem. - Eur. J.*, 2009, **15**, 9669-9673.
16. S.-L. Lee, C.-Y. J. Chi, M.-J. Huang, C.-h. Chen, C.-W. Li, K. Pati and R.-S. Liu, *J. Am. Chem. Soc.*, 2008, **130**, 10454-10455.
17. T. Balandina, K. Tahara, N. Sändig, M. O. Blunt, J. Adisoejoso, S. Lei, F. Zerbetto, Y. Tobe and S. De Feyter, *ACS Nano*, 2012, **6**, 8381-8389.
18. R. Addou and M. Batzill, *Langmuir*, 2013, **29**, 6354-6360.
19. J. Greenwood, T. H. Phan, Y. Fujita, Z. Li, O. Ivasenko, W. Vanderlinden, H. Van Gorp, W. Frederickx, G. Lu, K. Tahara, Y. Tobe, H. Uji-i, S. F. L. Mertens and S. De Feyter, *ACS Nano*, 2015, **9**, 5520-5535.
20. S. De Feyter, A. Gesquière, M. Klapper, K. Müllen and F. C. De Schryver, *Nano Letters*, 2003, **3**, 1485-1488.
21. F. Tao and S. L. Bernasek, *Surf. Sci.*, 2007, **601**, 2284-2290.
22. P. N. Dickerson, A. M. Hibberd, N. Oncel and S. L. Bernasek, *Langmuir*, 2010, **26**, 18155-18161.
23. K.-W. Park, J. Adisoejoso, J. Plas, J. Hong, K. Müllen and S. De Feyter, *Langmuir*, 2014, **30**, 15206-15211.
24. K. Kim, K. E. Plass and A. J. Matzger, *Langmuir*, 2003, **19**, 7149-7152.
25. Y. Fang, E. Ghijsens, O. Ivasenko, H. Cao, A. Noguchi, K. S. Mali, K. Tahara, Y. Tobe and S. De Feyter, *Nat. Chem.*, 2016, **8**, 711-717.